Earth and Planetary Science Letters 454 (2016) 282–292

Contents lists available at ScienceDirect

Earth and Planetary Science Letters

www.elsevier.com/locate/epsl

A new boron isotope-pH calibration for *Orbulina universa*, with implications for understanding and accounting for 'vital effects'

Michael J. Henehan [a,b,*], Gavin L. Foster [a], Helen C. Bostock [c], Rosanna Greenop [a,d], Brittney J. Marshall [e], Paul A. Wilson [a]

[a] Ocean and Earth Science, University of Southampton Waterfront Campus, National Oceanography Centre Southampton, European Way, Southampton SO14 3ZH, UK
[b] Department of Geology and Geophysics, Yale University, 210 Whitney Avenue, New Haven, CT-06511, USA
[c] National Institute for Water and Atmospheric Research, Evans Bay Parade, Wellington, New Zealand
[d] Department of Earth Sciences, Irvine Building, University of St. Andrews, St. Andrews KY16 9AL, Scotland, UK
[e] Department of Earth and Ocean Sciences, University of South Carolina, Columbia, SC 29208, USA

ARTICLE INFO

Article history:
Received 21 February 2016
Received in revised form 6 September 2016
Accepted 13 September 2016
Available online 4 October 2016
Editor: H. Stoll

Keywords:
boron isotopes
palaeo-CO_2
planktic foraminifera
vital effects
Orbulina universa

ABSTRACT

Boron isotope ratios, as measured in planktic foraminifera, can be a useful tracer of past ocean pH, and hence help to discern the concentration of CO_2 in the ancient atmosphere. However, different species of planktic foraminifera demonstrate different patterns of boron isotope variation with ambient seawater pH. Therefore when applying the proxy to questions in the geological past, species-specific calibrations are preferable. Beyond the evolutionary history of a calibrated species, we must rely on our understanding of the causes of the observed "vital effects" in the modern ocean, and the applicability of that understanding to extinct species. Here we present a new open-ocean calibration of the planktic foraminifera *Orbulina universa*, measured via Multi-Collector Inductively Coupled Mass Spectrometry (MC-ICPMS). Unlike other symbiont-bearing foraminifera, *O. universa* record a $\delta^{11}B$ (and hence pH) that is lower than its surrounding seawater, but with a pH-sensitivity roughly equal to that of aqueous borate ion. We discuss the significance of this for application of the boron isotope proxy in deep time, with recommendations for best practice and future research directions.

1. Introduction

The boron isotope-pH proxy (as applied to biogenic carbonates) is widely used for reconstructing palaeo-pH and past CO_2 concentrations. The proxy is based on the known pH-dependency of boron speciation in seawater, between boric acid, $B(OH)_3$, and the charged borate ion, $B(OH)_4^-$ (see Dickson, 1990). Because a known isotopic fractionation is associated with this speciation (Klochko et al., 2006), and because it is thought that the charged borate ion is the species incorporated into foraminiferal $CaCO_3$ (e.g. Branson et al., 2015; Hemming and Hanson, 1992; Rae et al., 2011), it is possible (with some additional parameters) to infer *in situ* pH from the boron isotopic composition (hereafter $\delta^{11}B$) of foraminiferal calcite (for a more detailed treatment, see Zeebe and Wolf-Gladrow, 2001; Foster and Rae, 2016). However, as with many other proxies (e.g. $\delta^{18}O$ and $\delta^{13}C$; Bemis et al., 1998; Bijma et al., 1998; Zeebe et al., 1999a) application of the boron isotope-pH proxy with confidence requires an understanding of how the physiology of the carbonate producer also influences the geochemical signatures recorded: so-called 'vital effects'. In the case of planktic foraminifera (commonly used to reconstruct surface ocean pH and atmospheric pCO_2), sizeable vital effects in $\delta^{11}B$ have been documented (e.g. Foster, 2008; Henehan et al., 2013; Hönisch et al., 2003; Martínez-Botí et al., 2015; Sanyal et al., 2001, 1996), with the magnitude and directionality (i.e. toward higher or lower $\delta^{11}B$) of these effects appearing to be species-specific. These vital effects are commonly explained as manifestations of an altered microenvironment around the foraminifera (Zeebe et al., 2003, 1999a). Microenvironment alterations arise because the immediate vicinity around a foraminiferal test is below the smallest scale of turbulent flow (also known as the Kolmogorov scale; Kolmogorov, 1991), and hence transport of nutrients, dissolved carbon species, etc. through this microenvironment is by diffusion only (Lazier and Mann, 1989). Because of the relatively slow equilibration and diffusion rates of dissolved carbon species (Zeebe et al., 1999b), the carbonate system within this diffusive boundary layer around a foraminifera may be different from the surrounding

* Corresponding author at: Department of Geology and Geophysics, Yale University, 210 Whitney Avenue, New Haven, CT-06511, USA.
E-mail address: Michael.Henehan@yale.edu (M.J. Henehan).

http://dx.doi.org/10.1016/j.epsl.2016.09.024

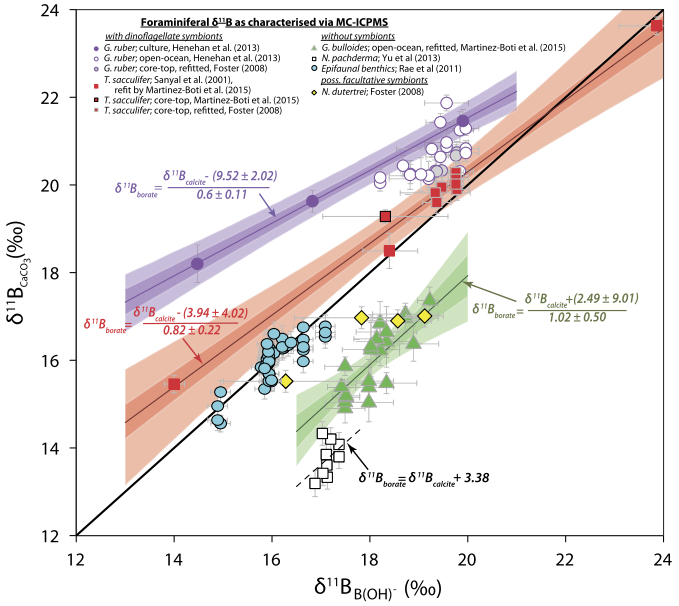

Fig. 1. Published boron isotope measurements in foraminiferal carbonates to data, as characterised by solution MC-ICPMS. To allow comparison of vital effects in isolation in an internally consistent dataset, NTIMS data are not plotted because of potentially variable laboratory-specific analytical offsets (Foster et al., 2013; Hönisch et al., 2003) between NTIMS datasets, with the exception of data from *T. sacculifer* (Sanyal et al., 2001) which has been corroborated by comparison with core-top MC-ICPMS measurements. Calibrations and bounds of uncertainty are calculated via combined Monte Carlo-wild bootstrap approach (see Section 2.4). The *T. sacculifer* calibration incorporates culture data (Sanyal et al., 2001) offset by −3.32‰ (see Fig. S2), as well as core-tops from Martínez-Botí et al. (2015) and Foster (2008). The *G. bulloides* calibration incorporates all core-tops from Martínez-Botí et al. (2015), including the Holocene measurement from Site PS2498-1 not originally included in that calibration dataset.

waters (Zeebe et al., 1999a) and the resultant pH offset causes the vital effects recorded in planktic foraminiferal δ^{11}B (Hönisch et al., 2003; Zeebe et al., 2003).

The release of CO_2 during respiration and calcification means that the foraminiferal microenvironment, in the absence of photosynthesising symbionts, should be lower in pH than the ambient seawater. In symbiont-bearing foraminifera, though, the carbonate system is also altered by the net uptake of DIC (probably mainly CO_{2aq}; Colman et al., 2002; Zeebe et al., 1999a) by photosynthesising symbionts. This may raise pH to the extent that the acidifying effects of host respiration and calcification are outweighed and the microenvironment around the foraminifera become more alkaline than ambient seawater (Zeebe et al., 2003, 1999a). There is abundant empirical evidence of these microenvironment perturbations from *in vitro* microelectrode measurements (Glas et al., 2012; Jørgensen et al., 1985; Köhler-Rink and Kühl, 2000, 2001, 2005; Rink et al., 1998). Importantly, inter-species differences in δ^{11}B are largely consistent with microenvironment-derived vital effects. For instance, symbiont-bearing taxa such as *Trilobatus* (formerly *Globigerinoides*) *sacculifer* (sensu Spezzaferri et al., 2015) and *Globigerinoides ruber* have been shown to record elevated δ^{11}B compared to ambient borate ion (Foster, 2008; Henehan et al., 2013; Sanyal et al., 2001), while symbiont-barren forms such as *Globigerina bulloides* and *Neogloboquadrina pachyderma* record lower δ^{11}B than ambient borate (Hönisch et al., 2003; Martínez-Botí et al., 2015; Yu et al., 2013) (Fig. 1). In addition, symbiont-bearing foraminifera grown in the dark, without symbiont photosynthetic activity, record lower δ^{11}B than those grown in the light (Hönisch et al., 2003). Among benthic foraminifera, larger symbiont-bearing species elevate the pH in their microenviroment (Glas et al., 2012; Köhler-Rink and Kühl, 2001) and similarly record above-ambient δ^{11}B (Rollion-Bard and Erez, 2010). Deep-sea epifaunal benthic foraminifera show no offset from ambient borate (Rae et al., 2011), consistent with low metabolic rates in these species (Nomaki et al., 2007), and a lack of microenvironment pH alteration observed around similar benthic species (Glas et al., 2012). In all these cases, striking agreement between δ^{11}B and observed microenvironment carbonate system alteration persists despite known internal upregulation of the pH of internal calcification pools (e.g. Bentov et al., 2009), and apparent non-equilibrium fractionation in inorganic calcites (Kaczmarek et al., 2016; Noireaux et al., 2015; Sanyal et al., 2000), suggesting models of boron isotope vital effects (Zeebe et al., 2003) are fundamentally well-founded. That said, there are still some inconsistencies between modelled vital effects and data. For instance, Zeebe et al. (2003) suggest that foraminiferal microenvironment-driven vital effects should be constant in magnitude regardless of ambient seawater pH, i.e. they may produce absolute offsets but do not affect pH sensitivity. Instead, we observe that in symbiont-bearing species calibrated to date (Henehan et al., 2013; Sanyal et al., 2001, 1996) foraminiferal δ^{11}B is increasingly positively offset from $\delta^{11}B_{borate}$ as ambient pH is lowered (see Fig. 1), i.e. pH-sensitivity of foraminiferal δ^{11}B is lower than that of aqueous borate ion. The same result is not seen for non-symbiont-bearing species (Martínez-Botí et al., 2015), suggesting that this phenomenon may be driven by symbionts, via a mechanism that is unaccounted for in previous models.

In addition, the offset in δ^{11}B between published culture calibrations of *T. sacculifer* (Sanyal et al., 2001) and *O. universa* (Sanyal et al., 1996) culture calibrations is too large (∼3‰) to be explained within the framework of current models (Zeebe et al., 2003). Were this offset the result of differences in microenvironment pH, it would imply a microenvironment pH in *T. sacculifer* >0.3 pH units higher than in *O. universa* (from Sanyal et al., 1996), and 0.25–0.3 pH units higher than in *G. ruber* (Henehan et al., 2013). This is incompatible with microelectrode observations of microenvironment pH in *O. universa* (Köhler-Rink and Kühl, 2005; Rink et al., 1998) and *T. sacculifer* (Jørgensen et al., 1985), even accounting for any potential differences in day:night calcification (Anderson and Faber, 1984; Lea et al., 1995), as discussed by Zeebe et al. (2003). It has however recently been recognised that some of this inconsistency stems from analytical inaccuracy of the earlier Negative Thermal Ionisation Mass Spectrometry (N-TIMS) work (Foster et al., 2013). Accounting for a laboratory-specific ∼3.3‰ positive bias due to analysis via NTIMS in this laboratory (Foster et al., 2012; Martínez-Botí et al., 2015) brings culture (Sanyal et al., 2001) and core-top (Sanyal et al., 1995) *T. sacculifer* into more proximal agreement with cultures of *G. ruber* measured via MC-ICPMS (Henehan et al., 2013), but the same analytical offset might then also be applicable to the calibration of Sanyal et al. (1996) for *O. universa* (Fig. S1). This would produce values of δ^{11}B in *O. universa* below those of ambient borate ion, which would suggest lowered microenvironment pH, counter to microelectrode observations (Köhler-Rink and Kühl, 2005; Rink et al., 1998). Here we address this apparent mismatch between *in vitro* observations and proxy measurements by constructing a new δ^{11}B-pH calibration of *O. universa* using MC-ICPMS measurements of open-ocean samples. As its name suggests, *O. universa* is a cosmopolitan species of planktic foraminifera, which together with its long fossil record (∼16 Ma), easily distinguishable morphology, well studied physiology (e.g. Hamilton et al., 2008; Hönisch et al., 2003; Köhler-Rink and Kühl, 2005; Lea et al., 1995; Rink et al., 1998; Spero, 1988; Spero and Parker, 1985; Vetter et al., 2013; Zeebe et al., 2003), and large test size could make it an ideal subject for down-core application of the boron isotope-pH proxy. By accurately characterising vital effects in this species and reconciling our findings with existing understanding of microenvironment alteration we provide a new tool in palaeo-pH and palaeo-CO_2 reconstruction. In addition, we present MC-ICPMS analyses of δ^{11}B

in open-ocean samples of several other symbiont-bearing, facultative symbiont-bearing, and symbiont-barren foraminifera to extend the range of characterised planktic foraminifera and provide better context for existing calibrations. In the light of these findings, we discuss the considerations that must be made when applying modern planktic foraminiferal calibrations in deep time, including how vital effects can be best characterised to permit more accurate palaeo-pH reconstructions.

2. Methods

2.1. Sample selection

Because *O. universa* is geographically widespread and lives across a wide range of ambient pH and hence $\delta^{11}B_{borate}$ it is possible to construct a viable boron isotope calibration without the requirement of culture experiments. Here we combine plankton tows, sediment trap and core-top samples to construct the first fully open-ocean calibration for *O. universa*. Plankton tow material was collected using a Multiple Opening and Closing Nets for Ecological Sub-Sampling (MOCNESS) apparatus (Wiebe et al., 1985) on board the *RV Tangaroa* (NIWA Cruise TAN1106, Solander Trough, April–May 2011; Bostock, 2011). The MOCNESS apparatus allowed for towing over tightly constrained depth ranges, with CTD bottle casts also taken at each site to determine hydrographic and carbonate system conditions. MOCNESS samples analysed here are from 0 to 50 m water depth (TAN1106/40) and 50 to 100 m water depth TAN1106/24 and TAN1106/50), and were towed at night. MOCNESS-collected foraminifera were separated from soft-bodied plankton using saturated NaCl solution, before being rinsed thoroughly in de-ionised water, dried at <50 °C for 24–48 hrs, sieved and picked. In addition, we analysed *O. universa* picked from material towed from <10 m water depth in the Gulf of Aqaba (Eilat) in Jan–March 2010.

Towed samples were complemented by sediment trap samples from the Cariaco Basin (CAR22(Z), positioned at 150 m water depth, and collected January 2007). In addition, core-top samples were selected to maximise the range in pH and aqueous $\delta^{11}B_{borate}$, and to sample from multiple ocean basins to investigate any possible regional effects (as noted in Mg/Ca; Marr et al., 2011). Measurements were also made on a number of size fractions to examine any influence of test size on measured $\delta^{11}B$ (as discussed by Hönisch and Hemming, 2004; Ni et al., 2007; Henehan et al., 2013).

In addition to measurements of *O. universa*, we measured samples of the shallow-dwelling obligate crysophycophyte-bearing spinose species *Globigerinella siphonifera* (*from tow, core-top*), non-spinose, merely facultative crysophycophyte-bearers *Globoconella inflata* (*tows, core-tops*) *and Pulleniatina obliquiloculata* (*core-top*), and the non-spinose, symbiont-barren *Neogloboquadrina pachyderma* (*core-top*). These species were sampled from sites where *O. universa* were also analysed, except in the case of *N. pachyderma*, where at that site the assemblage was almost monospecific. Size ranges for each species are listed in Table S1.

Core-top samples were from the archives at the University of Tübingen, Germany and NIWA, New Zealand. Samples from NIWA (J50 & ODP 1172C) were verified as recent by way of ^{14}C-dating (Cortese and Prebble, 2015), while from the Tübingen repository only undisturbed multicore samples containing Rose Bengal-stained living benthic foraminifera were used. The locations of core-top and sediment trap sites are shown in Fig. 2 (see also Table 1).

2.2. Calculating in situ $\delta^{11}B_{borate}$

As in Henehan et al. (2013), surface ocean pH was estimated for core-top sites using surface water oceanographic data from the

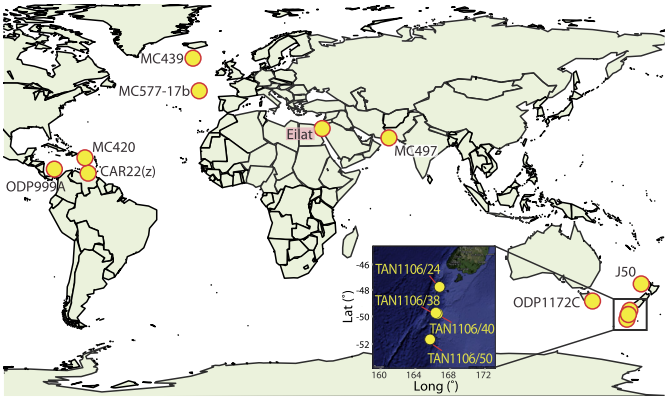

Fig. 2. Site locations for core-top, tow and sediment trap samples (see Table 1 for further details). The inset panel shows the locations of samples taken aboard the RV Tangaroa TAN1106-Solander Trough Cruise from NIWA, Wellington in April 2011.

GLODAP (Key et al., 2004), CARINA (Key et al., 2010) and Takahashi et al. (2009) databases. We use regional correlations of salinity and temperature with total alkalinity (TAlk) from Lee et al. (2006). Applying these correlations, monthly-resolved estimates of salinity and temperature from Takahashi et al. (2009) were converted to monthly TAlk estimates. Pre-industrial pCO_2 at each core-top site was estimated by applying monthly ocean-atmosphere disequilibrium (ΔpCO_2) from Takahashi et al. (2009) (corrected for the post-industrial changes in flux with reference to Gloor et al. (2003)) to a pre-industrial atmospheric pCO_2 value. Where samples were ^{14}C-dated, the age-appropriate atmospheric pCO_2 value was taken from Lüthi et al. (2008). Where core-tops were not dated, we assume an average late Holocene (<4 kyr BP) value of 275 ppm. Combined with approximations of typical local silicate and phosphate concentrations (from GLODAP/CARINA), monthly estimates of pH were calculated using CO2sys.m (van Heuven et al., 2011), the carbon constants of Lueker et al. (2000), boron to chlorinity ratio of Lee et al. (2010) and equilibrium constants of Dickson (1990).

For tow samples, $\delta^{11}B_{borate}$ is calculated from temperature, salinity, total alkalinity and dissolved inorganic carbon ([DIC]) measurements from each site. For TAN1106 MOCNESS samples, seawater was sampled with Niskin bottles on a CTD array, deployed close to each tow site and triggered at the approximate depths of each MOCNESS subsampling net. At each MOCNESS tow site, $\delta^{11}B_{borate}$ at the depth of sample nets was found to be within measurement uncertainty of surface conditions. For the Cariaco Basin, no CTD or carbonate system measurements are included in the Cariaco Time Series for the month when sediment trap samples were collected (January 2007). As such, $\delta^{11}B_{borate}$ is interpolated from pH, temperature and salinity values from adjacent monthly measurements in December 2006 and February 2007, downloadable from http://www.imars.usf.edu/CAR, assuming that no transient anomalous conditions arose within this time period. The total range of $\delta^{11}B_{borate}$ between these two months was then taken as uncertainty.

2.3. Analytical methods

Analytical methods are as discussed in Foster (2008), Foster et al. (2013) and Henehan et al. (2013). Sediment trap and tow sample specimens, following other culturing studies (e.g. Russell et al., 2004; Henehan et al., 2013), were subject to intensified oxidative cleaning (3 × 20–30 min treatments of 250 µl 1% H_2O_2 + 0.1 M NH_4OH at 80 °C) to account for the greater presence of organics. In core-tops, oxidative cleaning was shorter (3 × 5 min) to minimise sample loss. Al/Ca ratios were monitored for clay contamination and values >100 µmol/mol discounted. Uncertainty for most samples was calculated according to the external reproducibility of

Table 1
New Calibration data for *O. universa* plotted in Fig. 3. For details of the derivation of in situ conditions, see Section 2.2. Sample marked with ∗ was measured with 10^{12} Ω resistors, and so analytical reproducibility was estimated with Equation (2) (all others use Equation (1)). Age estimates for core-tops, and details of estimated in situ pCO_2, are given in Supplementary Table 2.

Sample type	Site	Latitude (°N)	Longitude (°E)	Size range (μm)	Temperature (°C)	±(2σ)	Salinity	±(2σ)	pH (total scale)	±(2σ)	$\delta^{11}B_{borate}$ (‰)	±(2σ)	$\delta^{11}B_{calcite}$ (‰)	±(2σ)
Core-top	ODP 1172C	−43.96	149.93	300–355	13.7	2.9	35.0	0.2	8.196	0.004	18.14	0.47	16.17	0.20
Core-top	MC577-17b	45.57	−17.40	300–355	15.3	4.8	35.7	0.1	8.188	0.002	18.34	0.62	16.97	0.21
MOCNESS Tow	TAN1106/24-Net8	−47.91	165.79	300–355	12.5	0.5	34.7	0.1	8.087	0.010	16.93	0.15	15.98	0.43
Core-top	TAN1106/38	−49.69	165.07	300–355	9.8	2.0	34.5	0.2	8.186	0.003	17.51	0.28	15.99	0.19
MOCNESS Tow	TAN1106/50-Net8	−51.71	164.56	300–355	9.0	0.5	34.4	0.0	8.056	0.010	16.28	0.15	15.15	0.17
MOCNESS Tow	TAN1106/40-Net9	−49.72	165.21	300–355	11.0	1.0	34.6	0.1	8.071	0.020	16.61	0.15	15.65	0.28
Core-top	MC439	59.46	−20.03	355–400	10.1	3.1	35.2	0.1	8.200	0.019	17.74	0.66	16.29	0.18
MOCNESS Tow	TAN1106/24-Net8	−47.91	165.79	355–400	12.5	0.5	34.7	0.1	8.087	0.010	16.93	0.15	15.84	0.40
MOCNESS Tow	TAN1106/50-Net8	−51.71	164.56	355–400	9.0	0.5	34.4	0.0	8.056	0.010	16.28	0.15	15.19	0.18
MOCNESS Tow	TAN1106/24-Net8	−47.91	165.79	400–450	12.5	0.5	34.7	0.1	8.087	0.010	16.93	0.15	16.08	0.23
Core-top	J50	−36.67	170.65	355–500	17.2	4.0	35.5	0.1	8.189	0.009	18.59	0.45	17.50	0.33
MOCNESS Tow	TAN1106/50-Net8	−51.71	164.56	>450	9.0	0.5	34.4	0.0	8.056	0.010	16.28	0.15	14.98	0.15
Sediment Trap	CAR22(z)	10.50	−64.66	500–600	24.2	2.0	36.7	0.1	8.076	0.035	18.21	0.10	16.62	0.19
Core-top	MC497	23.53	63.31	>355	26.9	3.6	36.4	0.2	8.152	0.020	19.57	0.45	18.04	0.27
Sediment Trap	CAR22(z)	10.50	−64.66	>600	24.2	2.0	36.7	0.1	8.076	0.035	18.21	0.10	16.82	0.20
Core-top	MC420	48.90	−12.10	355–400	27.6	1.1	35.5	0.5	8.168	0.013	19.82	0.05	18.57	0.28
Core-top	MC420	48.90	−12.10	>400	27.6	1.1	35.5	0.5	8.168	0.013	19.82	0.05	18.98	0.26
Core-top∗	ODP 999A	12.75	−78.73	400–500	27.9	1.0	35.8	0.3	8.158	0.019	19.76	0.16	18.82	0.20
Tow	Gulf of Aqaba (Eilat)	29.50	34.92	>500	23.0	0.5	40.4	0.1	8.116	0.002	18.78	0.24	19.47	0.31

repeat analyses of Japanese Geological Survey Porites coral standard (JCp-1, Inoue et al. (2004); $\delta^{11}B = 24.3 \pm 0.19‰$, 2σ) using 10^{11} Ω resistors at the University of Southampton, as described by

$$2\sigma = 1.87\left(e^{-20.69[^{11}B]}\right) + 0.22\left(e^{-0.43[^{11}B]}\right) \quad (1)$$

where $[^{11}B]$ is the observed beam intensity (in V) of ^{11}B (Henehan et al., 2013). However, three samples (marked with an asterisk in Tables 1 and S1) were analysed with 10^{12} Ω resistors, and so uncertainty is calculated according to equation (2) below, from Greenop et al. (2016).

$$2\sigma = 33450\left(e^{-168.2[^{11}B]}\right) + 0.311\left(e^{-1.477[^{11}B]}\right) \quad (2)$$

2.4. Calibration construction and uncertainty propagation

Calibration data (new and published) are described via linear regression between $\delta^{11}B_{borate}$ (*in situ*) and measured $\delta^{11}B_{calcite}$. In this way, data define straight lines with slopes reflecting the difference between the $\delta^{11}B$-pH sensitivity of $\delta^{11}B_{borate}$ and $\delta^{11}B_{calcite}$. Slopes and intercepts of these lines are independent of pK_B^* (and hence salinity, temperature and pressure), allowing comparison of geographically-disparate calibration data on one calibration curve without the complications introduced from variable *in situ* temperatures and salinities between samples, that would preclude presentation on traditional $\delta^{11}B$-pH plots.

A Monte Carlo approach was used to construct the calibration regression equation and its bounds of uncertainty, in R (R Core Team, 2015). One thousand simulated datasets were created, with a value of $\delta^{11}B_{calcite}$ randomly generated from within normal frequency distributions around quoted sample measurements (Tables 1 and S1), with standard deviations according to analytical reproducibility from equations (1) or (2) above. Similarly, random values for $\delta^{11}B_{borate}$ were generated from within bounds of two standard deviations of intra-annual variability at this site (core-tops) or from a conservative approximation of *in situ* measurement uncertainty (cultures, tows, sediment trap). Confidence intervals (1 and 2σ) on the calibration are then calculated using a wild bootstrap approach (Liu, 1988; Mammen, 1993). This avoids problems that can arise when utilising traditional bootstrap resampling to construct confidence intervals on small datasets (e.g. Cameron et al., 2008). In wild bootstrapping, predictor variables are fixed and the regression t-statistic is resampled instead (following Imbens and Kolesar, 2012, section A2, not imposing the null). For each Monte Carlo-simulated dataset, 500 wild bootstrap replicates of calibration slope and intercept were generated, using *sandwich* (Zeileis, 2004). The mean and 2 standard deviations of the 50,000 simulated regression parameters were then taken as the quoted value and 95% confidence intervals respectively. Note these analyses were carried out for both new and published datasets, and so regression equations and 95% confidence intervals in Figs. 1 and 4 may differ from previously published values where bootstrap approaches were not used. The advantage of this approach over previous studies is that it is an attempt to fully propagate the analytical uncertainty into the determination of the regression coefficients.

3. Results

3.1. Boron isotope calibration

Calibration data for *O. universa* are given in Table 1 and are plotted in Fig. 3. $\delta^{11}B$ data are lower than that of ambient borate ($B(OH)_4^-$) ion, and plot below the 1:1 line (with a mean offset of 1.24‰). The slope of the regression is almost unity (0.95 ± 0.08 and 0.17 at 68% and 95% confidence respectively), suggesting that

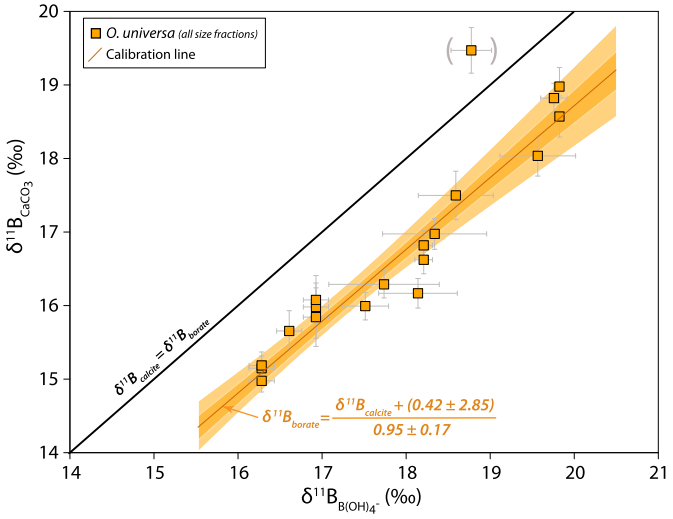

Fig. 3. A new calibration for *Orbulina universa*. $\delta^{11}B_{borate}$ is the estimated *in situ* boron isotopic composition of borate ion, according to adjacent hydrographic measurements from CTD casts (for MOCNESS tow material) or at estimated surface-water conditions (sediment traps, core-tops); see Section 2.2 for details.

open ocean *O. universa* display a pH-sensitivity roughly equal to that of aqueous borate ion. Scatter is low (for ordinary least squares regression the residual standard error is 0.31, $R^2 = 0.94$, $p < 0.0001$), with bounds of uncertainty on the calibration comparing favourably to other published calibrations. While we include tow and trap data in the calibration in Fig. 3 to maximise sample size, we tested the potential for differences stemming from the absence of gametogenic calcite in tow material, and the possible presence of non-gametogenic *O. universa* in Cariaco sediment trap samples (Marshall et al., 2015). The slopes of calibrations constructed without MOCNESS tows (1.18 ± 0.28) or without tow and trap samples (1.18 ± 0.29) do not vary outside of uncertainty from the slope of either the bulk calibration (0.95 ± 0.17) or borate ion (i.e. 1), suggesting the calibration is not significantly biased by inclusion of mixed sample types. However, this calibration line does exclude one data point (Cook's Distance = 0.5), shown in parentheses in Fig. 3: a towed sample of *O. universa* from the Gulf of Aqaba that recorded anomalous $\delta^{11}B$, elevated relative to ambient $B(OH)_4^-$. This data-point is discussed further in section 4.2. In addition, *G. siphonifera, N. pachyderma, P. obliquiloculata* and *G. inflata* (Table S1) all record lower $\delta^{11}B$ than that of ambient borate ($B(OH)_4^-$) ion (Fig. 4).

3.2. Investigating influence from other non-carbonate system factors

These data show no change in the offset between recorded $\delta^{11}B$ and ambient $\delta^{11}B_{borate}$ with either salinity or temperature, beyond the well understood effect on pK_B^* that is intrinsic in the calculation of $\delta^{11}B_{borate}$ (Fig. 5a,b), confirming overwhelming carbonate system control on the boron isotope pH proxy. Moreover, unlike in other symbiont-bearing planktic species (e.g. Henehan et al., 2013; Hönisch and Hemming, 2004) there is no apparent increase in $\delta^{11}B$ observed with increasing test size: within any one site all size fractions give the same value (within analytical uncertainty, see Fig. 5c).

4. Discussion

4.1. Acidification of the microenvironment in a symbiont-bearing foraminifera

The new $\delta^{11}B$ calibration for *O. universa* presented here is well constrained within the limitations of field calibration, thanks in

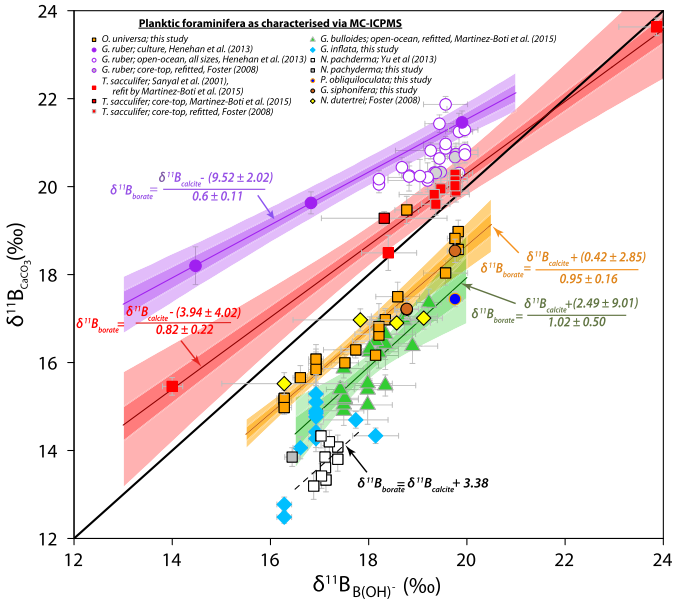

Fig. 4. Collated solution MC-ICPMS measurements of planktic foraminifera to date, demonstrating the considerable variability of vital effects observed amongst different species. Note that while more data exist from other analytical techniques (e.g. Hönisch et al., 2009; Sanyal et al., 1996), as in Fig. 1 we avoid plotting data where analytical offsets are not fully quantifiable, so as to permit comparison of internally consistent datasets. We plot these other datasets in Fig. S3. Shaded regions are calculated regions of uncertainty (1 and 2σ) on published calibration data. Note, these bounds of uncertainty account for the number of samples included in the calibration, which is why 2σ uncertainty in the *G. ruber* calibration of Henehan et al. (2013), which does not include core-top measurements of variable size, appears much larger than others listed. Error bars are as published, or for new data are 2σ uncertainty on analytical reproducibility (from Equation (1)) and 2σ uncertainty on *in situ* $\delta^{11}B_{borate}$ estimated reflecting intra-annual variability (core-tops; *N. pachyderma, O. universa, G. inflata, G. siphonifera, P. obliquiloculata*), measurement uncertainty (tows; *G. siphonifera, O. universa*), range between bracketing CTD measurements (MOCNESS samples; *O. universa, G. inflata*) or bracketing bimonthly hydrographic measurements (sediment trap; *O. universa*). Size ranges for each datapoint are listed in Table 1 and Supplementary Table 1.

part to the broad geographic (and thus *in situ* $\delta^{11}B_{borate}$) range of this species. It is, however, offset below the 1:1 line in Fig. 2; that is to say that it records lower $\delta^{11}B$ (and by implication pH, see Fig. S1) than *in situ* ocean carbonate system conditions predict. This seems at odds with micro-electrode observations of higher-than-ambient pH in the microenvironment of this species (Rink et al., 1998; Köhler-Rink and Kühl, 2005), and with microenvironment models for *O. universa* that derive in part from these observations (Zeebe et al., 2003, 1999a). Comparison with existing data, however, is not straightforward, since data from different NTIMS laboratories can be offset from each other (Hönisch et al., 2009, 2003) and from MC-ICPMS data (Foster et al., 2013). That said, if we tentatively apply the $\sim -3.3‰$ analytical offset observed in nearby core-top measurements of *T. sacculifer* (Foster et al., 2012; Martínez-Botí et al., 2015) versus those analysed at Stonybrook (Sanyal et al., 2001) the calibration of Sanyal et al. (1996; slope $= 0.77 \pm 0.23$, as later corroborated by Hönisch et al., 2009) comes into approximate agreement with our new calibration (slope $= 0.95 \pm 0.17$; see Fig. S2 and Fig. S3), which supports our findings. Recent laser ablation MC-ICPMS data from cultured *O. universa* (Howes et al., 2016) are also for the most part within uncertainty of our calibration line (see Fig. S3), albeit tending toward higher $\delta^{11}B$ than our open ocean samples. The causes of this offset are not currently clear, but might relate to *O. universa* in the Howes et al. (2016) study being grown in $10 \times [B]_{sw}$ which could conceivably act to buffer respiration-driven microenvironment acidification.

We suggest that lowered $\delta^{11}B$ in our *O. universa* calibration derives from microenvironment acidification that arises despite the presence of photosynthetic symbionts, as a result of a deeper habitat in this species compared to that of *T. sacculifer* or *G. ruber*. Although often referred to as a surface/mixed-layer species, *O. universa* is often found at deeper depths, even approaching the thermocline (Fairbanks et al., 1980; Spero and Williams, 1988; Sautter and Thunell, 1991; Marshall et al., 2015; Hemleben and Bijma, 1994). Indeed, in our MOCNESS tows, high incidence of *O. universa* was observed at depths of up to ~150 m (see Fig. S4). Similarly Morard et al. (2009) found live *O. universa* in MOCNESS tows from 100–200 m depth. For *T. sacculifer*, the 'photosynthetic compensation depth' (i.e. the depth at which photosynthetic activity is not high enough to cancel out the acidifying effects of respiration and calcification) is estimated at only 45 m water depth (Jørgensen et al., 1985). Therefore, it is likely that the degree of microenvironment pH elevation via photosynthetic symbionts in open-ocean *O. universa* is not only less than in *G. ruber* or *T. sacculifer*, but may be entirely cancelled out by respiration and calcification due to its deeper habitat depth. Maximum photosynthetic rate (P_{max}) for *O. universa* is at 386 µEinst m^2 s^{-1} (Spero and Parker, 1985). While Spero and Williams (1989) calculated a typical depth of approximately 40 m for these light levels (assuming

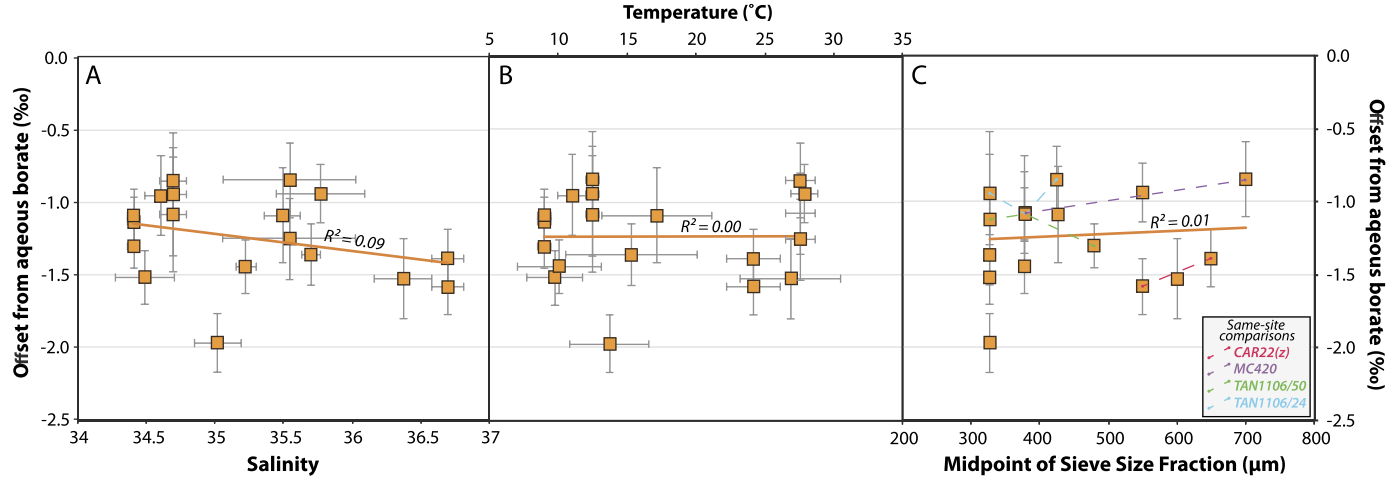

Fig. 5. No correlation between (a) salinity, (b) temperature or (c) size and the deviation of *O. universa* $\delta^{11}B$ from *in situ* $\delta^{11}B_{borate}$. Note that in all cases the anomalous measurement from the Gulf of Aqaba (Eilat) is excluded. Coloured dashed lines in panel C link samples from different size fractions measured at the same site, with no single-site comparison demonstrating coherent trends with size outside of analytical reproducibility. The latter finding is also shown in Fig. 6. (For interpretation of the colours in this figure, the reader is referred to the web version of this article.)

a light attenuation coefficient of 0.04 per m from Tyler, 1975), in the region of our MOCNESS tows the light attenuation coefficient is 0.07–0.1 m^{-1}. Consequently light levels drop to 1% of surface irradiance at depths of between 43 to 70 m (Howard-Williams et al., 1995). As such it is probable that MOCNESS tow material analysed here experienced irradiation levels below those required to compensate for the acidifying effects of respired CO_2. If this hypothesis is correct, the small amount of residual scatter around our new calibration might indicate that *O. universa* has an active preference for a certain light level. More empirical data on depth preferences of open-ocean *O. universa* elsewhere would help to test this hypothesis further.

This hypothesis also suggests that high levels of irradiance *in vitro* (under which conditions micro-electrode pH experiments were made) may not accurately simulate the light levels more commonly experienced by *O. universa* in the open ocean. Indeed, Hönisch et al. (2003) report that towed *O. universa* match more closely the $\delta^{11}B$ of individuals grown under low-light conditions (in which symbiont photosynthesis is minimal and microenvironment pH and $\delta^{11}B_{borate}$ should be lowered by respiration) than those grown under saturated light conditions (under which photosynthesis should significantly raise microenvironment pH and $\delta^{11}B_{borate}$), supporting this hypothesis. While core-top measurements by Sanyal et al. (1996) are in agreement with their culture calibration (and their calibration agrees approximately with ours when analytical offsets are accounted for) their culture experiments were performed without any additional illumination beyond normal laboratory ceiling lighting (Hönisch et al., 2003), so it is likely that irradiance levels in their cultures was below P_{max}, and that incident light was not of wavelengths favourable to photosynthesis (e.g. McCree, 1971). In this way, photosynthetically-active radiation in their cultures might be more comparable to those seen at depth by open ocean *O. universa*. As a mechanism to explain vital effects in $\delta^{11}B$ in *O. universa*, respiration-driven acidification of the microenvironment could also be compatible with the relatively higher $\delta^{11}B$ (compared to our measurements) observed in those culturing experiments where [B] is elevated, and hence seawater buffering capacity is greater (Hönisch et al., 2003; Howes et al., 2016).

Although an overriding control of light availability is well supported by the available data, an alternative possibility is that specific differences in timing of calcification may exist between *O. universa* and other symbiont-bearing foraminifera, such that *O. universa* precipitates more of its shell in darkness (when host and symbiont respiration lowers microenvironment pH) than in day time. Evidence, for this, however, is lacking. Although Lea et al. (1995) report ratios of day:night calcification of 3:1 (suggesting most calcification would take place in a high-pH microenvironment), recent studies of day:night banding in *O. universa* (Vetter et al., 2013) show roughly equal quantities of $CaCO_3$ precipitated during day and night (based on the thickness of bands). Also, maximum photosynthetic rates in *O. universa* are not reached until midday (Spero and Parker, 1985) so although $CaCO_3$ precipitated before this point may perhaps still be considered 'day' calcite (Lea et al., 1995) it may still record a microenvironment where respiration outweighs photosynthesis. However, because microenvironment pH elevation in saturated light ($\sim +0.6$) outweighs pH reduction in the dark (~ -0.15) by approximately 4:1 (Köhler-Rink and Kühl, 2005), the vast majority of $CaCO_3$ would have to be precipitated in the night to produce the average pH offset of -0.13 pH units we observe here. Moreover, the disagreement between studies, as well as variability of day:night calcification ratios observed by Lea et al. (1995), suggests that day:night calcification ratios are not fixed, and may differ within individuals of the same species. Therefore we tentatively suggest that differences in habitat depth may be a more straightforward explanation for the observed patterns.

It is worth noting that the slope of our new calibration (i.e. the pH sensitivity of $\delta^{11}B$ in *O. universa*) is close to 1 (Fig. 3). That is to say that, as in *G. bulloides* (Martínez-Botí et al., 2015) and in *Cibicidoides* (Rae et al., 2011), there is no significant deviation from the pH-sensitivity of $\delta^{11}B_{borate}$ indicated by a fractionation factor ($^{11\text{-}10}K_B$) of 1.0272 (Klochko et al., 2006). It is unclear why this differs in other symbiont-bearing species calibrated to date (Henehan et al., 2013; Sanyal et al., 2001), but we suggest it may indicate that the overall stronger photosynthetic activity of symbionts in *G. ruber* and *T. sacculifer* not only produces an absolute offset of foraminiferal $\delta^{11}B$ from that of ambient borate, but may also lower its pH sensitivity. In other words, it may imply that symbionts buffer the microenvironment of these species to an increasing degree as bulk seawater pH decreases.

Finally, recent observation of elevated $\delta^{11}B$ in inorganic calcite precipitates, but not in aragonite, has been interpreted as an indication that both aqueous species (boric acid and borate) may be incorporated into calcite (Noireaux et al., 2015). However, since *O. universa* (and numerous other species; Fig. 4) record lower $\delta^{11}B$ than that of aqueous borate, these data do not support incorporation of boric acid during precipitation of foraminiferal $CaCO_3$. It is possible, then, that inorganic precipitation experiments (often precipitated from non-seawater solution chemistries) do not effectively approximate conditions of natural biogenic precipitation. Clearly further investigation is required to ascertain the cause of this disagreement and allow greater confidence in the fundamentals of the proxy.

4.2. Anomalous results from the Red Sea

While the offset between the *O. universa* calibration of Sanyal et al. (1996) and the one presented here might be explained by analytical differences (Fig. S2), there remains an inconsistency within our MC-ICPMS data. One measurement from *O. universa* towed from the Gulf of Aqaba (Eilat) is considerably offset from other calibration data (by $\sim +2‰$; Fig. 3). Given that there is no correlation elsewhere between salinity and deviation from aqueous $\delta^{11}B_{borate}$ within a range of salinity of 34.4 and 36.7 (Fig. 5a) it seems unlikely that this is related to the unusually high salinity levels (>40) seen in the Gulf of Aqaba (Eilat). Moreover the tight correlation in other tow and core-top data (Fig. 3) suggests that regional differences in productivity and nutrient availability at most have only limited effects on $\delta^{11}B$. Unusual seawater chemistry could have some effect on ion pairing and equilibrium constants (Hain et al., 2015) but major ion chemistry in the northern Gulf of Aqaba (Eilat) is not drastically different here compared to elsewhere (Friedman, 1968; Steiner et al., 2014), and so is insufficiently unusual to significantly alter equilibrium constants. Given morphotype-specific variations observed in $\delta^{18}O$ (Deuser et al., 1981; Marshall et al., 2015), some disparity in recorded $\delta^{11}B$ could conceivably be linked to the presence of some different cryptic species of *O. universa* in the Gulf of Aqaba (Eilat). Three genotypes (Types I, II and III) of *O. universa* have been defined on the basis of small subunit (SSU) mRNA (Darling and Wade, 2008; de Vargas et al., 1999), corresponding to three specific morphotypes (Deuser et al., 1981; Marshall et al., 2015; Morard et al., 2009). It is possible that boron isotope variations may exist between these genotypes, given their offset in $\delta^{18}O$ and $\delta^{13}C$ (Marshall et al., 2015). However, in the Gulf of Aqaba (Eilat) region, the Type III 'high-productivity' (or Mediterranean-type; Morard et al., 2009) genotype are found. Given that Type III is also the genotype most prevalent in other regions sampled in this study (Darling and Wade, 2008), it seems difficult to explain the observed dichotomy of $\delta^{11}B$ signals through cryptospecies variations. Indeed the tight correlation in our data

may suggest at most limited differences in δ^{11}B between cryptospecies, despite evident differences in δ^{18}O and δ^{13}C (Marshall et al., 2015).

More likely, perhaps, is that habitat depth is driving observed patterns, as a result of associated changes in irradiance. In Eilat, *O. universa* were collected from <10 m water depth, in a region where the euphotic zone stretches to 115 m water depth, and light attenuation is low (Stambler, 2006). In this way, our tows from Eilat may have preferentially sampled individuals from high-light environments (where the effect of symbiont photosynthesis is strongest) before any ontogenetic migration to depth had taken place. As such it is probable that $CaCO_3$ analysed from these tows experienced irradiation levels well above those required to compensate for the acidifying effects of respired CO_2. That said, Hönisch et al. (2003) towed *O. universa* from depths of <20 m, where irradiance was still likely above the light compensation for *O. universa*, yet these specimens still recorded 'dark'-type δ^{11}B signals, which would require these individuals to have recently migrated up from depth.

4.3. Implications: microenvironment alteration in deep time

These data are the first data from symbiont-bearing foraminifera that record lower δ^{11}B, and hence pH, than ambient seawater, and serve as a cautionary example that symbiosis, often inferred in extinct species from relatively heavy δ^{13}C signatures, may not necessarily imply elevation of microenvironment pH. That said, since these *O. universa* data are still heavier in δ^{11}B than symbiont-barren species *G. bulloides* (by ~1 to 1.5‰; the same offset observed by Hönisch et al., 2003) and *N. pachyderma* (Martínez-Botí et al., 2015; Yu et al., 2013; this study), some effect of symbiont photosynthesis is still evident (see Fig. 4). We note also that the shallow-dwelling obligate crysophycophyte-bearing spinose species *G. siphonifera* appears to demonstrate patterns in δ^{11}B similar to *O. universa* (Fig. 4), although with the proviso that these were not separated by morphotype (type I or II; Bijma et al., 1998). In contrast, non-spinose, merely facultative crysophycophyte-bearers such as *G. inflata, P. obliquiloculata* and *N. dutertrei* (Hemleben et al., 1989), are more variable and often record δ^{11}B values more similar to symbiont-barren species (e.g. *G. bulloides* or *N. pachyderma*; Fig. 4). There is, therefore, an increasingly congruent picture emerging from comparison of this and other published data from symbiont-bearing and symbiont-barren foraminifera: that respiration of planktic foraminifera acidifies the microenvironment around a foraminifera, and that photosynthetic symbionts may counteract this acidification to a greater or lesser degree, depending on factors such as symbiont type or strength of symbiont photosynthetic activity (in turn a function of symbiont density and depth habitat relative to photosynthetic compensation point). Among those foraminifera bearing large dinoflagellate symbionts, the magnitude of vital effects track typical habitat depth (Bijma et al., 1992; Erez and Honjo, 1981), with δ^{11}B in *G. ruber* > *T. sacculifer* > *O. universa*.

While this more nuanced view of the effect of symbiosis on δ^{11}B presents a potential challenge to palaeo-applications using extinct species, by measuring a suite of isotope (δ^{11}B, δ^{13}C and δ^{18}O) and trace element ratios (e.g. B/Ca, Mg/Ca) across a transect of the broader planktic foraminiferal assemblage, it may still be possible to infer ecologically/physiologically analogous modern species and apply appropriate calibrations to extinct assemblages. For example, variation in δ^{13}C between size fractions within a species, and in comparison to other species, can imply the presence or absence of symbionts and even the type of symbionts present (Ezard et al., 2015 and references within). Comparison of δ^{18}O between extinct species may then be useful in constraining growth temperature (e.g. Erez and Honjo, 1981) and hence relative habitat depth,

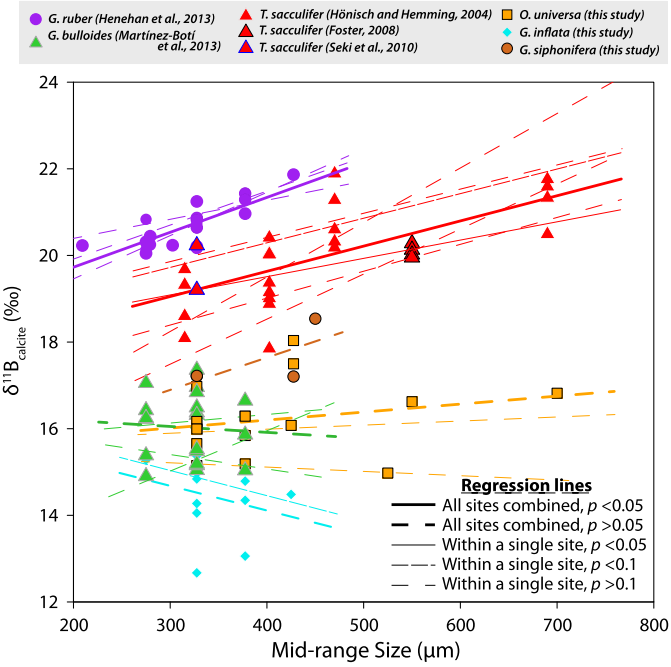

Fig. 6. Distribution of δ^{11}B versus test size in Holocene samples of six planktic foraminiferal species. Thick lines are regression lines plotted through all individuals of a species, with dashed lines signifying non-significant regressions and solid lines marking statistically significant ($p < 0.05$) regression lines. Within each species set, where three or more size fractions were measured at any one site, regression lines are plotted through these data to illustrate the degree of consistency of trends within species across sites. These thinner lines are plotted as either solid (statistically significant regressions, $p < 0.05$), densely dashed ($p < 0.1$), or sparsely dashed (non-significant, $p > 0.1$). Test size, for the purpose of plotting, is marked as the mid-range of quoted sieve sizes, except in the case of three tows of *G. ruber* from Eilat, where known means of measured major axes are used.

irradiance levels, and likely vital effects. In addition, increases in δ^{11}B with size-fraction may further indicate the strength of symbiont influence on the microenvironment. In modern species, these size-related changes are only observed in *G. ruber* (Henehan et al., 2013), and (less strongly) in *T. sacculifer* (Foster, 2008; Hönisch and Hemming, 2004; Seki et al., 2010): both species that record elevated δ^{11}B/pH relative to ambient seawater. In contrast, in species where respiration dominates signals of microenvironment alteration (Martínez-Botí et al., 2015, this study), or where microenvironment effects are negligible (Rae et al., 2011), no significant size-related trends are observed in δ^{11}B (see Fig. 6). While further work is no doubt required to ascertain the physiological basis for these observed trends, correlations between size and δ^{11}B may prove useful in assigning appropriate calibrations when combined with other indicators.

Across an assemblage, comparison of δ^{11}B between species (with depth habitat for each species inferred from Mg/Ca or δ^{18}O), may also help to constrain vital effects. For example, large offsets in δ^{11}B between species living at similar temperatures (i.e. habitat depths), for example, may by necessity imply the presence or absence of symbionts, and the magnitude of this offset can permit comparison with modern calibrations and interspecies offsets. Finally, it is possible that B/Ca ratios may also be used to infer aspects of symbiont ecology. Empirically, in the modern ocean, planktic foraminiferal B/Ca ratios largely mirror the magnitude and direction of vital effects in δ^{11}B, even though the controls on B incorporation may be complex (e.g. Henehan et al., 2015). In both open ocean (Fig. 7) and cultured foraminifera (Allen et al., 2012), [B] is highest in *G. ruber* (that shows the largest vital effects in δ^{11}B), followed by *T. sacculifer* (also offset to more positive δ^{11}B), followed by *O. universa* and other species whose vital effects ap-

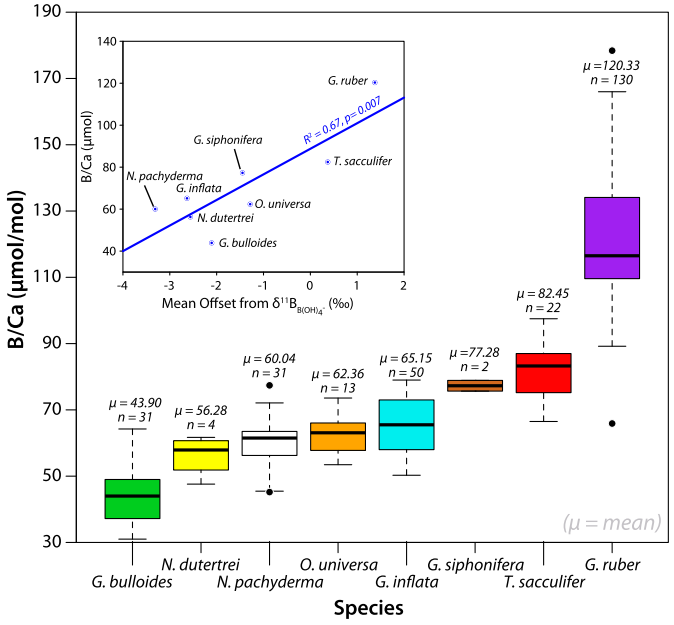

Fig. 7. Collated distributions of measured B/Ca ratios in Holocene planktic foraminifera. Means of each species' B/Ca ratios are significantly positively correlated with vital effects in δ^{11}B observed in open-ocean samples via MC-ICPMS (see inset). B/Ca data are from this study [*O. universa, N. pachyderma, G. inflata, G. siphonifera, G. bulloides*], Henehan et al. (2015) [*G. ruber*], Babila et al. (2014) [*G. ruber*], Foster (2008) [*G. ruber, T. sacculifer, N. dutertrei*], Ni et al. (2007) [*G. ruber, T. sacculifer*], Seki et al. (2010) [*T. sacculifer*], Yu et al. (2007) [*G. inflata, G. bulloides*], Yu et al. (2013) [*N. pachyderma*] and Hendry et al. (2009) [*N. pachyderma*]. Mean offsets from $\delta^{11}B_{borate}$ for each species are calculated from this study, Henehan et al. (2013), Martínez-Botí et al. (2015), Yu et al. (2013), Seki et al. (2010), and Foster (2008).

pear to be predominantly respiration-driven (Fig. 7). Just as with size driven changes in δ^{11}B discussed above, there remains a clear need for a mechanistic understanding of the drivers of these vital effects in both B/Ca and δ^{11}B to permit full confidence in absolute reconstructions of pH and pCO_2 from extinct species. However, through combination of these more qualitative, empirically-based indicators with more quantitative palaeoecological signals across multiple geochemical proxy systems, we suggest it is still possible to make informed approximations of the nature of vital effects in extinct species.

5. Conclusions

This contribution resolves some inconsistencies between previous planktic foraminiferal calibrations and *in vitro* observations, and provides further support for the importance of microenvironment alteration in dictating foraminiferal vital effects. Our new calibration for *O. universa* provides one of the most tightly-constrained calibration of any species to date, derived from open-ocean samples without risk of artefacts from culture. Better understanding of foraminiferal autecology and seasonality in the open ocean could in future constrain such calibrations still further. Together with apparently negligible size-fraction or cryptospecies effects in δ^{11}B and this species' broad geographic range, long fossil record, and large and easily recognisable morphology, this calibration should prove a very useful tool for reconstruction of past pH and pCO_2. In addition, through comparison with new and published measurements of other foraminiferal species, an increasingly congruent picture of the nature of foraminiferal vital effects is emerging. Although ultimately more advanced models of foraminiferal microenvironment alteration and biomineralisation – grounded in more extensive physiological and geochemical measurements – are needed, we outline some practical solutions to allow approximation of vital effects in extinct species. These approaches, we suggest, may permit greater confidence in absolute values of ocean pH and atmospheric pCO_2 calculated from the δ^{11}B of extinct foraminiferal species, thereby extending the utility of the boron isotope-pH proxy.

Acknowledgements

We thank Jonathan Erez for helpful comments and insights lent during drafting of this manuscript. We thank the other members of the B-Team at the University of Southampton for valuable discussion and assistance in the laboratory. We thank Lisa Northcote (NIWA) for foraminiferal assemblage counts in MOCNESS tows, Kim Currie (NIWA) for DIC and Alkalinity analyses, and the crew and research staff on board the RV Tangaroa Cruise TAN1106, including Kevin McGill and Peter Gerring for assistance with MOCNESS operations. Michal Kucera and the staff at the University of Tübingen are thanked for provision of core-top sample material from their archives. Michael Weaver (Yale) provided valuable assistance with quantification of calibration uncertainty. We acknowledge Bob Thunnell, the Fundación La Salle de Ciencias Naturales, Estación de Investigaciones Marinas Isla Margarita (EDIMAR) and the crew of the R/V Hermano Ginés for provision of CARIACO Time Series material and data. We also thank Bärbel Hönisch for enlightening discussion with regard to vital effects in the species discussed here. This work was aided by NERC PhD studentships granted to MH and RG, and NERC grant NE/D00876X/2 awarded to GF. Voyage TAN1106 was funded by the New Zealand government through NIWA core funding, and Cariaco sampling was funded through NSF award 1258991. This research used samples from the Ocean Drilling Program. We thank J. Bijma and one anonymous reviewer for their constructive comments.

Appendix A. Supplementary material

Supplementary material related to this article can be found online at http://dx.doi.org/10.1016/j.epsl.2016.09.024.

References

Allen, K.A., Hönisch, B., Eggins, S.M., Rosenthal, Y., 2012. Environmental controls on B/Ca in calcite tests of the tropical planktic foraminifer species Globigerinoides ruber and Globigerinoides sacculifer. Earth Planet. Sci. Lett. 351–352, 270–280. http://dx.doi.org/10.1016/j.epsl.2012.07.004.

Anderson, O.R., Faber, W.W.J., 1984. An estimation of calcium carbonate deposition rate in a planktonic foraminifer Globigerinoides sacculifer using Ca-45 as a tracer – a recommended procedure for improved accuracy. J. Foraminiferal Res. 14, 303–308.

Babila, T.L., Rosenthal, Y., Conte, M.H., 2014. Evaluation of the biogeochemical controls on B/Ca of Globigerinoides ruber white from the Oceanic Flux Program, Bermuda. Earth Planet. Sci. Lett. 404, 67–76. http://dx.doi.org/10.1016/j.epsl.2014.05.053.

Bemis, B.E., Spero, H.J., Bijma, J., Lea, D.W., 1998. Reevaluation of the oxygen isotopic composition of planktonic foraminifera: experimental results and revised paleotemperature equations. Paleoceanography 13, 150–160. http://dx.doi.org/10.1029/98PA00070.

Bentov, S., Brownlee, C., Erez, J., 2009. The role of seawater endocytosis in the biomineralization process in calcareous foraminifera. Proc. Natl. Acad. Sci. 106, 21500–21504. http://dx.doi.org/10.1073/pnas.0906636106.

Bijma, J., Hemleben, C., Huber, B.T., Erlenkeuser, H., Kroon, D., 1998. Experimental determination of the ontogenetic stable isotope variability in two morphotypes of Globigerinella siphonifera (d'Orbigny). Mar. Micropaleontol. 35, 141–160. http://dx.doi.org/10.1016/S0377-8398(98)00017-6.

Bijma, J., Hemleben, C., Oberhaensli, H., Spindler, M., 1992. The effects of increased water fertility on tropical spinose planktonic foraminifers in laboratory cultures. J. Foraminiferal Res. 22, 242–256. http://dx.doi.org/10.2113/gsjfr.22.3.242.

Bostock, H., 2011. TAN1106- Solander Trough (Unpublished voyage report), National Institute of Water and Atmospheric Research, Wellington.

Branson, O., Kaczmarek, K., Redfern, S.A.T., Misra, S., Langer, G., Tyliszczak, T., Bijma, J., Elderfield, H., 2015. The coordination and distribution of B in foraminiferal calcite. Earth Planet. Sci. Lett. 416, 67–72. http://dx.doi.org/10.1016/j.epsl.2015.02.006.

Cameron, A.C., Gelbach, J.B., Miller, D.L., 2008. Bootstrap-based improvements for inference with clustered errors. Rev. Econ. Stat. 90, 414–427. http://dx.doi.org/10.1162/rest.90.3.414.

Colman, B., Huertas, I.E., Bhatti, S., Dason, J.S., 2002. The diversity of inorganic carbon acquisition mechanisms in eukaryotic microalgae. Funct. Plant Biol. 29, 261–270.

Cortese, G., Prebble, J., 2015. A radiolarian-based modern analogue dataset for palaeoenvironmental reconstructions in the southwest Pacific. Mar. Micropaleontol. 118, 34–49. http://dx.doi.org/10.1016/j.marmicro.2015.05.002.

Darling, K.F., Wade, C.M., 2008. The genetic diversity of planktic foraminifera and the global distribution of ribosomal RNA genotypes. Mar. Micropaleontol. 67, 216–238. http://dx.doi.org/10.1016/j.marmicro.2008.01.009.

Deuser, W.G., Ross, E.H., Hemleben, C., Spindler, M., 1981. Seasonal changes in species composition, numbers, mass, size, and isotopic composition of planktonic foraminifera settling into the deep Sargasso Sea. Palaeogeogr. Palaeoclimatol. Palaeoecol. 33, 103–127.

de Vargas, C., Norris, R., Zaninetti, L., Gibb, S.W., Pawlowski, J., 1999. Molecular evidence of cryptic speciation in planktonic foraminifers and their relation to oceanic provinces. Proc. Natl. Acad. Sci. 96, 2864–2868. http://dx.doi.org/10.1073/pnas.96.6.2864.

Dickson, A.G., 1990. Thermodynamics of the dissociation of boric acid in synthetic seawater from 273.15 to 318.15 K. Deep-Sea Res., A, Oceanogr. Res. Pap. 37, 755–766. http://dx.doi.org/10.1016/0198-0149(90)90004-F.

Erez, J., Honjo, S., 1981. Comparison of isotopic composition of planktonic foraminifera in plankton tows, sediment traps and sediments. Palaeogeogr. Palaeoclimatol. Palaeoecol. 33, 129–156. http://dx.doi.org/10.1016/0031-0182(81)90035-3.

Ezard, T.H.G., Edgar, K.M., Hull, P.M., 2015. Environmental and biological controls on size-specific $\delta^{13}C$ and $\delta^{18}O$ in recent planktonic foraminifera: synthesising size-specific $\delta^{13}C$ and $\delta^{18}O$. Paleoceanography 30, 151–173. http://dx.doi.org/10.1002/2014PA002735.

Fairbanks, R.G., Wiebe, P.H., Bé, A.W.H., 1980. Vertical distribution and isotopic composition of living planktonic foraminifera in the Western North Atlantic. Science 207, 61–63. http://dx.doi.org/10.1126/science.207.4426.61.

Foster, G.L., 2008. Seawater pH, pCO_2 and [CO_2-3] variations in the Caribbean Sea over the last 130 kyr: a boron isotope and B/Ca study of planktic foraminifera. Earth Planet. Sci. Lett. 271, 254–266. http://dx.doi.org/10.1016/j.epsl.2008.04.015.

Foster, G.L., Hönisch, B., Paris, G., Dwyer, G.S., Rae, J.W.B., Elliott, T.R., Gaillardet, J., Hemming, N.G., Louvat, P., Vengosh, A., 2013. Interlaboratory comparison of boron isotope analyses of boric acid, seawater and marine $CaCO_3$ by MC-ICPMS and NTIMS. Chem. Geol. 358, 1–14. http://dx.doi.org/10.1016/j.chemgeo.2013.08.027.

Foster, G.L., Lear, C.H., Rae, J.W.B., 2012. The evolution of pCO_2, ice volume and climate during the middle Miocene. Earth Planet. Sci. Lett. 341–344, 243–254. http://dx.doi.org/10.1016/j.epsl.2012.06.007.

Foster, G.L., Rae, J.W.B., 2016. Reconstructing ocean pH with boron isotopes in foraminifera. Annu. Rev. Earth Planet. Sci. 44, 207–237. http://dx.doi.org/10.1146/annurev-earth-060115-012226.

Friedman, G.M., 1968. Geology and geochemistry of reefs, carbonate sediments, and waters, Gulf of Aqaba (Elat), Red Sea. SEPM J. Sediment. Res. 38. http://dx.doi.org/10.1306/74D71AAA-2B21-11D7-8648000102C1865D.

Glas, M.S., Fabricius, K.E., de Beer, D., Uthicke, S., 2012. The O_2, pH and Ca_2+ microenvironment of benthic foraminifera in a high CO_2 world. PLoS ONE 7, e50010. http://dx.doi.org/10.1371/journal.pone.0050010.

Gloor, M., Gruber, N., Sarmiento, J., Sabine, C.L., Feely, R.A., Rödenbeck, C., 2003. A first estimate of present and preindustrial air-sea CO_2 flux patterns based on ocean interior carbon measurements and models. Geophys. Res. Lett. 30, 1010. http://dx.doi.org/10.1029/2002GL015594.

Greenop, R., Foster, G.L., Sosdian, S., Hain, M.P., Oliver, K.I.C., Goodwin, P., Chalk, T.B., Lear, C.H., Wilson, P.A., 2016. A record of Neogene seawater $\delta^{11}B$ reconstructed from paired $\delta^{11}B$ analyses on benthic and planktic foraminifera. Clim. Past Discuss. http://dx.doi.org/10.5194/cp-2015-177, in press.

Hain, M.P., Sigman, D.M., Higgins, J.A., Haug, G.H., 2015. The effects of secular calcium and magnesium concentration changes on the thermodynamics of seawater acid/base chemistry: implications for Eocene and Cretaceous ocean carbon chemistry and buffering. Glob. Biogeochem. Cycles 2014GB004986. http://dx.doi.org/10.1002/2014GB004986.

Hamilton, C.P., Spero, H.J., Bijma, J., Lea, D.W., 2008. Geochemical investigation of gametogenic calcite addition in the planktonic foraminifera Orbulina universa. Mar. Micropaleontol. 68, 256–267. http://dx.doi.org/10.1016/j.marmicro.2008.04.003.

Hemleben, C., Bijma, J., 1994. Foraminiferal population dynamics and stable carbon isotopes. In: Zahn, R., Pedersen, T.F., Kaminski, M.A., Labeyrie, L. (Eds.), Carbon Cycling in the Glacial Ocean: Constraints on the Ocean's Role in Global Change. Springer, Berlin, Heidelberg, pp. 145–166.

Hemleben, C., Spindler, M., Erson, O.R., 1989. Modern Planktonic Foraminifera. Springer, Berlin.

Hemming, N.G., Hanson, G.N., 1992. Boron isotopic composition and concentration in modern marine carbonates. Geochim. Cosmochim. Acta 56, 537–543. http://dx.doi.org/10.1016/0016-7037(92)90151-8.

Hendry, K.R., Rickaby, R.E.M., Meredith, M.P., Elderfield, H., 2009. Controls on stable isotope and trace metal uptake in Neogloboquadrina pachyderma (sinistral) from an Antarctic sea-ice environment. Earth Planet. Sci. Lett. 278, 67–77. http://dx.doi.org/10.1016/j.epsl.2008.11.026.

Henehan, M.J., Foster, G.L., Rae, J.W.B., Prentice, K.C., Erez, J., Bostock, H.C., Marshall, B.J., Wilson, P.A., 2015. Evaluating the utility of B/Ca ratios in planktic foraminifera as a proxy for the carbonate system: a case study of Globigerinoides ruber: investigating controls on G. ruber B/Ca. Geochem. Geophys. Geosyst. 16, 1052–1069. http://dx.doi.org/10.1002/2014GC005514.

Henehan, M.J., Rae, J.W.B., Foster, G.L., Erez, J., Prentice, K.C., Kucera, M., Bostock, H.C., Martínez-Botí, M.A., Milton, J.A., Wilson, P.A., Marshall, B.J., Elliott, T., 2013. Calibration of the boron isotope proxy in the planktonic foraminifera Globigerinoides ruber for use in palaeo-CO_2 reconstruction. Earth Planet. Sci. Lett. 364, 111–122. http://dx.doi.org/10.1016/j.epsl.2012.12.029.

Hönisch, B., Bijma, J., Russell, A.D., Spero, H.J., Palmer, M.R., Zeebe, R.E., Eisenhauer, A., 2003. The influence of symbiont photosynthesis on the boron isotopic composition of foraminifera shells. Mar. Micropaleontol. 49, 87–96. http://dx.doi.org/10.1016/S0377-8398(03)00030-6.

Hönisch, B., Hemming, N.G., 2004. Ground-truthing the boron isotope-paleo-pH proxy in planktonic foraminifera shells: partial dissolution and shell size effects. Paleoceanography 19, 13. http://dx.doi.org/10.1029/2004PA001026.

Hönisch, B., Hemming, N.G., Archer, D., Siddall, M., McManus, J.F., 2009. Atmospheric carbon dioxide concentration across the mid-Pleistocene transition. Science 324, 1551–1554. http://dx.doi.org/10.1126/science.1171477.

Howard-Williams, C., Davies-Colley, R., Vincent, W.F., 1995. Optical properties of the coastal and oceanic waters off South Island, New Zealand: regional variation. N.Z. J. Mar. Freshw. Res. 29, 589–602. http://dx.doi.org/10.1080/00288330.1995.9516690.

Howes, E.L., Kaczmarek, K., Raitzsch, M., Mewes, A., Bijma, N., Horn, I., Misra, S., Gattuso, J.-P., Bijma, J., 2016. Decoupled carbonate chemistry controls on the incorporation of boron into Orbulina universa. Biogeosci. Discuss., 1–26. http://dx.doi.org/10.5194/bg-2016-90.

Imbens, G.W., Kolesar, M., 2012. Robust standard errors in small samples: some practical advice. (Working paper No. 18478). National Bureau of Economic Research.

Inoue, M., Nohara, M., Okai, T., Suzuki, A., Kawahata, H., 2004. Concentrations of trace elements in carbonate reference materials coral JCp-1 and Giant Clam JCt-1 by inductively coupled plasma-mass spectrometry. Geostand. Geoanal. Res. 28, 411–416. http://dx.doi.org/10.1111/j.1751-908X.2004.tb00759.x.

Jørgensen, B.B., Erez, J., Revsbech, N.P., Cohen, Y., 1985. Symbiotic photosynthesis in a planktonic foraminiferan, globigerinoides sacculifer (Brady), studied with microelectrodes. Limnol. Oceanogr. 30, 1253–1267.

Kaczmarek, K., Nehrke, G., Misra, S., Bijma, J., Elderfield, H., 2016. Investigating the effects of growth rate and temperature on the B/Ca ratio and $\delta^{11}B$ during inorganic calcite formation. Chem. Geol. 421, 81–92. http://dx.doi.org/10.1016/j.chemgeo.2015.12.002.

Key, R.M., Kozyr, A., Sabine, C.L., Lee, K., Wanninkhof, R., Bullister, J.L., Feely, R.A., Millero, F.J., Mordy, C., Peng, T.-H., 2004. A global ocean carbon climatology: results from Global Data Analysis Project (GLODAP). Glob. Biogeochem. Cycles 18, 23. http://dx.doi.org/10.1029/2004GB002247.

Key, R.M., Tanhua, T., Olsen, A., Hoppema, M., Jutterström, S., Schirnick, C., van Heuven, S., Kozyr, A., Lin, X., Velo, A., Wallace, D.W.R., Mintrop, L., 2010. The CARINA data synthesis project: introduction and overview. Earth Syst. Sci. Data 2, 105–121.

Klochko, K., Kaufman, A.J., Yao, W., Byrne, R.H., Tossell, J.A., 2006. Experimental measurement of boron isotope fractionation in seawater. Earth Planet. Sci. Lett. 248, 276–285. http://dx.doi.org/10.1016/j.epsl.2006.05.034.

Köhler-Rink, S., Kühl, M., 2005. The chemical microenvironment of the symbiotic planktonic foraminifer Orbulina universa. Marine Biol. Res. 1, 68–78. http://dx.doi.org/10.1080/17451000510019015.

Köhler-Rink, S., Kühl, M., 2001. Microsensor studies of photosynthesis and respiration in the larger symbiont bearing foraminifera Amphistegina lobifera, and Amphisorus hemprichii. Ophelia 55, 111–122. http://dx.doi.org/10.1080/00785236.2001.10409478.

Köhler-Rink, S., Kühl, M., 2000. Microsensor studies of photosynthesis and respiration in larger symbiotic foraminifera. I The physico-chemical microenvironment of Marginopora vertebralis, Amphistegina lobifera and Amphisorus hemprichii. Mar. Biol. 137, 473–486. http://dx.doi.org/10.1007/s002270000335.

Kolmogorov, A.N., 1991. Dissipation of energy in the locally isotropic turbulence. Proc. R. Soc., Math. Phys. Eng. Sci. 434, 15–17. http://dx.doi.org/10.1098/rspa.1991.0076.

Lazier, J.R.N., Mann, K.H., 1989. Turbulence and the diffusive layers around small organisms. Deep-Sea Res., A, Oceanogr. Res. Pap. 36, 1721–1733. http://dx.doi.org/10.1016/0198-0149(89)90068-X.

Lea, D.W., Martin, P.A., Chan, D.A., Spero, H.J., 1995. Calcium uptake and calcification rate in the planktonic foraminifer Orbulina universa. J. Foraminiferal Res. 25, 14–23. http://dx.doi.org/10.2113/gsjfr.25.1.14.

Lee, K., Kim, T.-W., Byrne, R.H., Millero, F.J., Feely, R.A., Liu, Y.-M., 2010. The universal ratio of boron to chlorinity for the North Pacific and North Atlantic oceans. Geochim. Cosmochim. Acta 74, 1801–1811. http://dx.doi.org/10.1016/j.gca.2009.12.027.

Lee, K., Tong, L.T., Millero, F.J., Sabine, C.L., Dickson, A.G., Goyet, C., Park, G.-H., Wanninkhof, R., Feely, R.A., Key, R.M., 2006. Global relationships of total alkalinity with salinity and temperature in surface waters of the world's oceans. Geophys. Res. Lett. 33, 19605.

Liu, R.Y., 1988. Bootstrap procedures under some non-iid models. Ann. Stat. 16, 1696–1708.

Lueker, T.J., Dickson, A.G., Keeling, C.D., 2000. Ocean pCO_2 calculated from dissolved inorganic carbon, alkalinity, and equations for K1 and K2: validation based on laboratory measurements of CO_2 in gas and seawater at equilibrium. Mar. Chem. 70, 105–119. http://dx.doi.org/10.1016/S0304-4203(00)00022-0.

Lüthi, D., Le Floch, M., Bereiter, B., Blunier, T., Barnola, J.-M., Siegenthaler, U., Raynaud, D., Jouzel, J., Fischer, H., Kawamura, K., Stocker, T.F., 2008. High-resolution carbon dioxide concentration record 650,000–800,000 years before present. Nature 453, 379–382. http://dx.doi.org/10.1038/nature06949.

Mammen, E., 1993. Bootstrap and wild bootstrap for high dimensional linear models. Ann. Stat. 21, 255–285.

Marr, J.P., Baker, J.A., Carter, L., Allan, A.S.R., Dunbar, G.B., Bostock, H.C., 2011. Ecological and temperature controls on Mg/Ca ratios of Globigerina bulloides from the southwest Pacific Ocean. Paleoceanography 26, 15. http://dx.doi.org/10.1029/2010PA002059.

Marshall, B.J., Thunell, R.C., Spero, H.J., Henehan, M.J., Lorenzoni, L., Astor, Y., 2015. Morphometric and stable isotopic differentiation of Orbulina universa morphotypes from the Cariaco Basin, Venezuela. Mar. Micropaleontol. http://dx.doi.org/10.1016/j.marmicro.2015.08.001.

Martínez-Botí, M.A., Marino, G., Foster, G.L., Ziveri, P., Henehan, M.J., Rae, J.W.B., Mortyn, P.G., Vance, D., 2015. Boron isotope evidence for oceanic carbon dioxide leakage during the last deglaciation. Nature 518, 219–222. http://dx.doi.org/10.1038/nature14155.

McCree, K.J., 1971. The action spectrum, absorptance and quantum yield of photosynthesis in crop plants. Agric. For. Meteorol. 9, 191–216. http://dx.doi.org/10.1016/0002-1571(71)90022-7.

Morard, R., Quillévéré, F., Escarguel, G., Ujiie, Y., de Garidel-Thoron, T., Norris, R.D., de Vargas, C., 2009. Morphological recognition of cryptic species in the planktonic foraminifer Orbulina universa. Mar. Micropaleontol. 71, 148–165. http://dx.doi.org/10.1016/j.marmicro.2009.03.001.

Ni, Y., Foster, G.L., Bailey, T., Elliott, T.R., Schmidt, D.N., Pearson, P., Haley, B., Coath, C., 2007. A core top assessment of proxies for the ocean carbonate system in surface-dwelling foraminifers. Paleoceanography 22, 3212–3226. http://dx.doi.org/10.1029/2006PA001337.

Noireaux, J., Mavromatis, V., Gaillardet, J., Schott, J., Montouillout, V., Louvat, P., Rollion-Bard, C., Neuville, D.R., 2015. Crystallographic control on the boron isotope paleo-pH proxy. Earth Planet. Sci. Lett. 430, 398–407. http://dx.doi.org/10.1016/j.epsl.2015.07.063.

Nomaki, H., Yamaoka, A., Shirayama, Y., Kitazato, H., 2007. Deep-sea benthic foraminiferal respiration rates measured under laboratory conditions. J. Foraminiferal Res. 37, 281–286. http://dx.doi.org/10.2113/gsjfr.37.4.281.

Rae, J.W.B., Foster, G.L., Schmidt, D.N., Elliott, T., 2011. Boron isotopes and B/Ca in benthic foraminifera: proxies for the deep ocean carbonate system. Earth Planet. Sci. Lett. 302, 403–413. http://dx.doi.org/10.1016/j.epsl.2010.12.034.

R Core Team, 2015. R: A Language and Environment for Statistical Computing. R Foundation for Statistical Computing, Vienna, Austria.

Rink, S., Kühl, M., Bijma, J., Spero, H.J., 1998. Microsensor studies of photosynthesis and respiration in the symbiotic foraminifer Orbulina universa. Mar. Biol. 131, 583–595.

Rollion-Bard, C., Erez, J., 2010. Intra-shell boron isotope ratios in the symbiont-bearing benthic foraminiferan Amphistegina lobifera: implications for [delta]11B vital effects and paleo-pH reconstructions. Geochim. Cosmochim. Acta 74, 1530–1536. http://dx.doi.org/10.1016/j.gca.2009.11.017.

Russell, A.D., Hönisch, B., Spero, H.J., Lea, D.W., 2004. Effects of seawater carbonate ion concentration and temperature on shell U, Mg, and Sr in cultured planktonic foraminifera. Geochim. Cosmochim. Acta 68, 4347–4361. http://dx.doi.org/10.1016/j.gca.2004.03.013.

Sanyal, A., Bijma, J., Spero, H.J., Lea, D.W., 2001. Empirical relationship between pH and the boron isotopic composition of Globigerinoides sacculifer: implications for the boron isotope paleo-pH proxy. Paleoceanography 16, 515–519.

Sanyal, A., Hemming, N.G., Broecker, W.S., Lea, D.W., Spero, H.J., Hanson, G.N., 1996. Oceanic pH control on the boron isotopic composition of foraminifera: evidence from culture experiments. Paleoceanography 11, 513–517.

Sanyal, A., Hemming, N.G., Hanson, G.N., Broecker, W.S., 1995. Evidence for a higher pH in the glacial ocean from boron isotopes in foraminifera. Nature 373, 234–236. http://dx.doi.org/10.1038/373234a0.

Sanyal, A., Nugent, M., Reeder, R.J., Bijma, J., 2000. Seawater pH control on the boron isotopic composition of calcite: evidence from inorganic calcite precipitation experiments. Geochim. Cosmochim. Acta 64, 1551–1555. http://dx.doi.org/10.1016/S0016-7037(99)00437-8.

Sautter, L.R., Thunell, R.C., 1991. Seasonal variability in the $\delta^{18}O$ and $\delta^{13}C$ of planktonic foraminifera from an upwelling environment: sediment trap results from the San Pedro Basin, southern California Bight. Paleoceanography 6, 307–334. http://dx.doi.org/10.1029/91PA00385.

Seki, O., Foster, G.L., Schmidt, D.N., Mackensen, A., Kawamura, K., Pancost, R.D., 2010. Alkenone and boron-based Pliocene pCO_2 records. Earth Planet. Sci. Lett. 292, 201–211.

Spero, H.J., 1988. Ultrastructural examination of chamber morphogenesis and biomineralization in the planktonic foraminifer Orbulina universa. Mar. Biol. 99, 9–20. http://dx.doi.org/10.1007/BF00644972.

Spero, H.J., Parker, S.L., 1985. Photosynthesis in the symbiotic planktonic foraminifer Orbulina universa, and its potential contribution to oceanic primary productivity. J. Foraminiferal Res. 15, 273–281. http://dx.doi.org/10.2113/gsjfr.15.4.273.

Spero, H.J., Williams, D.F., 1989. Opening the carbon isotope "vital effect" black box 1. Seasonal temperatures in the euphotic zone. Paleoceanography 4, 593–601. http://dx.doi.org/10.1029/PA004i006p00593.

Spero, H.J., Williams, D.F., 1988. Extracting environmental information from planktonic foraminiferal $\delta^{13}C$ data. Nature 335, 717–719. http://dx.doi.org/10.1038/335717a0.

Spezzaferri, S., Kucera, M., Pearson, P.N., Wade, B.S., Rappo, S., Poole, C.R., Morard, R., Stalder, C., 2015. Fossil and genetic evidence for the polyphyletic nature of the planktonic foraminifera "globigerinoides", and description of the new genus trilobatus. PLoS ONE 10, e0128108. http://dx.doi.org/10.1371/journal.pone.0128108.

Stambler, N., 2006. Light and picophytoplankton in the Gulf of Eilat (Aqaba). J. Geophys. Res. 111. http://dx.doi.org/10.1029/2005JC003373.

Steiner, Z., Erez, J., Shemesh, A., Yam, R., Katz, A., Lazar, B., 2014. Basin-scale estimates of pelagic and coral reef calcification in the Red Sea and Western Indian Ocean. Proc. Natl. Acad. Sci. 111, 16303–16308. http://dx.doi.org/10.1073/pnas.1414323111.

Takahashi, T., Sutherland, S.C., Wanninkhof, R., Sweeney, C., Feely, R.A., Chipman, D.W., Hales, B., Friederich, G., Chavez, F., Sabine, C., et al., 2009. Climatological mean and decadal change in surface ocean pCO_2, and net sea–air CO_2 flux over the global oceans. Deep-Sea Res., Part 2, Top. Stud. Oceanogr. 56, 554–577.

Tyler, J.E., 1975. The in situ quantum efficiency of natural phytoplankton populations. Limnol. Oceanogr. 20, 976–980. http://dx.doi.org/10.4319/lo.1975.20.6.0976.

van Heuven, S., Pierrot, D., Rae, J.W.B., Lewis, E., Wallace, D.W.R., 2011. MATLAB Program Developed for CO_2 System Calculations., CO_2 sys. Carbon Dioxide Information Analysis Center, Oak Ridge National Laboratory, U.S.

Vetter, L., Kozdon, R., Mora, C.I., Eggins, S.M., Valley, J.W., Hönisch, B., Spero, H.J., 2013. Micron-scale intrashell oxygen isotope variation in cultured planktic foraminifers. Geochim. Cosmochim. Acta 107, 267–278. http://dx.doi.org/10.1016/j.gca.2012.12.046.

Wiebe, P.H., Morton, A.W., Bradley, A.M., Backus, R.H., Craddock, J.E., Barber, V., Cowles, T.J., Flierl, G.R., 1985. New development in the MOCNESS, an apparatus for sampling zooplankton and micronekton. Mar. Biol. 87, 313–323. http://dx.doi.org/10.1007/BF00397811.

Yu, J., Elderfield, H., Hönisch, B., 2007. B/Ca in planktonic foraminifera as a proxy for surface seawater pH. Paleoceanography 22, PA2202. http://dx.doi.org/10.1029/2006PA001347.

Yu, J., Thornalley, D.J.R., Rae, J.W.B., McCave, I.N., 2013. Calibration and application of B/Ca, Cd/Ca and $\delta^{11}B$ in Neogloboquadrina pachyderma (sinistral) to constrain CO_2 uptake in the subpolar North Atlantic during the last deglaciation. Paleoceanography 28, 237–252. http://dx.doi.org/10.1002/palo.20024.

Zeebe, R.E., Bijma, J., Wolf-Gladrow, D.A., 1999a. A diffusion-reaction model of carbon isotope fractionation in foraminifera. Mar. Chem. 64, 199–227. http://dx.doi.org/10.1016/S0304-4203(98)00075-9.

Zeebe, R.E., Wolf-Gladrow, D.A., 2001. CO_2 in Seawater: Equilibrium, Kinetics, Isotopes. Elsevier Oceanography Series. Elsevier, Amsterdam.

Zeebe, R.E., Wolf-Gladrow, D.A., Bijma, J., Hönisch, B., 2003. Vital effects in foraminifera do not compromise the use of $\delta^{11}B$ as a paleo-pH indicator: evidence from modeling: Cretaceous marine temperature evolution. Paleoceanography 18. http://dx.doi.org/10.1029/2003PA000881.

Zeebe, R.E., Wolf-Gladrow, D.A., Jansen, H., 1999b. On the time required to establish chemical and isotopic equilibrium in the carbon dioxide system in seawater. Mar. Chem. 65, 135–153.

Zeileis, A., 2004. Econometric computing with HC and HAC covariance matrix estimators. J. Stat. Softw. 11, 1–17. http://dx.doi.org/10.18637/jss.v011.i10.